FLEXURAL BEHAVIOR OF PROTECTED CONCRETE SLABS AFTER FIRE EXPOSURE

M.A. Youssef*, S.F. El-Fitiany, and M.A. Elfeki

Department of Civil and Environmental Engineering, The University of Western Ontario,
London, ON, Canada N6A 5B9

Biography:

ACI member **M.A. Youssef** is an assistant professor at The University of Western Ontario. Dr. Youssef received his Ph.D. in Civil Engineering from McMaster University, Hamilton, Ontario. His research interests include: modeling of reinforced concrete structures, fire resilience of concrete structures, use of innovative materials (Fibre Reinforced Polymers, FRP, and Shape Memory Alloys, SMA) to upgrade the capacity of existing structures, using SMA to minimize structural damage during earthquakes, and seismic capacity of existing structures.

ACI student member **S.F. El-Fitiany** is a MESc candidate at The University of Western Ontario, Canada. Mr. El-Fitiany obtained his BSc from Alexandria University, Egypt. His research interests include Behavior of structures during and after exposure to fire and development of performance based fire design approaches.

ACI student member **M.A. Elfeki** is a PhD candidate at the University of Western Ontario, Canada. Mr. Elfeki obtained his BSc and MSc from Alexandria University, Egypt. His research interests include: seismic analysis, rehabilitation of concrete structures using Shape Memory Alloys, and fire testing.

* Corresponding author: E-mail: youssef@uwo.ca, Phone: 519-661-2111 Ext. 88661

ABSTRACT

Fire is one of the common events that might occur during the lifetime of any concrete structure. At elevated temperatures, mechanical properties of concrete and reinforcing bars experience significant deterioration. Following a fire event, these properties improve with time toward their original values. The paper focuses on the flexural behavior of unreinforced or lightly reinforced siliceous concrete slabs after exposure to elevated temperatures. Such behavior is controlled by the concrete tensile behavior. Models to predict related concrete and steel mechanical properties during and after exposure to elevated temperatures are presented. When needed, new models are developed based on available experiments data. A case study involving flexural testing of eleven concrete slabs after 85 days from exposure to fire is presented. The slabs were protected by a Thin Sprayed Liner (TSL). The case study allowed evaluating the presented models and assessing the effect of the TSL layer on the slabs behavior.

Keywords: Concrete; elevated temperatures; mechanical properties; strength regain; post-cooling; tensile behavior; stress-strain relationship; fire; slab.

INTRODUCTION

Designing concrete structures for fire exposure and evaluating the condition of fire-damaged concrete structures are research topics that received significant attention by many researchers[1-4]. Fire affects concrete structures by generating a heat flow that initiates at the exposed surfaces and produces high temperatures and pore pressure gradients within the concrete mass. When concrete is subjected to such a condition, its properties including compressive strength, tensile strength, and initial modulus of elasticity deteriorate[1-4]. The level of deterioration is influenced by aggregate type, temperature level, heating rate, applied loading, and external sealing[5, 6]. After

extinguishing a fire, concrete properties improve with time toward their original values[6-9]. Fire temperatures also result in marked changes in concrete strains. It increases strains required for equilibrium by shifting the value of the strain corresponding to peak stress[2]. It also introduces new strains, transient and thermal[2, 3]. Changes in concrete properties due to fire temperatures are dependent on the level of preloading[2, 3, 10].

The flexural behavior of unreinforced or lightly reinforced concrete slabs is mainly controlled by the concrete tensile behavior. The most common method for measuring the tensile strength of concrete involves testing unreinforced concrete beams according to ASTM C78[11]. This paper reviews the available work on siliceous concrete properties affecting its tensile behavior during heating, cooling, and post-cooling stages. These properties are used to develop estimates for the concrete tensile behavior at each of these stages. Based on these estimates, a tensile stress strain relationship is proposed.

As a case study, eleven siliceous concrete slabs sprayed with a TSL layer were tested in flexure after 85 days from fire exposure. These slabs were constructed and exposed to fire at the side coated with the TSL layer. Flexural tests were conducted on two groups of slabs with the TSL layer either in compression or in tension. The case study allowed examining the proposed material models and assessing the effect of the TSL layer on the behavior of the slabs.

RESEARCH SIGNIFICANCE

Fire-damaged concrete elements are usually assessed using destructive and/or non-destructive field tests. However, there are no design guidelines to help designers predict the overall behavior of a fire-damaged structure. Few experimental investigations can be found in the literature addressing concrete residual compressive capacity after fire exposure. A review of the analytical and experimental work related to the concrete tensile behavior is presented in this paper.

Formulas to predict the concrete tensile stress-strain relationships are proposed. The paper provides essential knowledge for structural engineers to judge on the safety of unreinforced or lightly reinforced fire-damaged concrete members.

CONCRETE COMPRESSIVE STRENGTH

Concrete compressive strength at elevated temperatures, $(f'_{cT})_{t=0}$, can be evaluated experimentally by heating unloaded or loaded concrete specimens and testing the hot concrete in compression. The time t is measured from the day concrete was exposed to fire. To evaluate the residual compressive strength, $(f'_{cT})_t$, specimens are cooled-down before testing. The following sections trace changes in $(f'_{cT})_t$ as the time t increases.

Heating Stage

Concrete compressive strength experiences a large reduction at temperatures above 300 °C [572 °F][4], **Fig. 1a** at $t = 0$. This reduction is caused by the complete evaporation of chemically bound water, the decomposition of the calcium hydroxide crystals CH at 400-600 °C [752-1112 °F], and the full destruction of the gel structure C-S-H at 900 °C [1652 °F][4, 7]. Several numerical models were developed by different researchers to estimate $(f'_{cT})_{t=0}$. A review of these models is given by Youssef and Moftah[2] and resulted in recommending Hertz model[4], Eq. (1).

$$(f'_{cT})_{t=0} = \frac{f'_c}{1+\frac{T}{15{,}000}+\left(\frac{T}{800}\right)^2+\left(\frac{T}{570}\right)^8+\left(\frac{T}{100{,}000}\right)^{64}} \quad (1)$$

Where T is the elevated temperature in degree Celsius [T °C = (T °F -32)×5/9] and f'_c is the siliceous concrete compressive strength at ambient temperature.

Heating loaded concrete specimens reduces the effect of fire temperature on its compressive strength. Applied external loads act as crack-development inhibitors. Hertz[4] reported that preloading siliceous concrete specimens with a stress level ($\lambda_L = f_c / f'_c$) of 0.25 to 0.30 results in 25% increase in $(f'_{cT})_{t=0}$ for temperatures between 500 °C and 700 °C [932 °F and 1292 °F].

Cooling Stage

$(f'_{cT})_t$ is greatly affected by the type of the cooling process. Rapid cooling, such as quenching in water, result in filling the micro-cracks formed during the heating stage by new hydration products and thus $(f'_{cT})_t$ increases upon cooling. On the other hand, slow cooling results in widening the micro-cracks[4] due to the relative hydration expansion between the moist outer layer and the dry inner core[6] and thus $(f'_{cT})_t$ decreases upon cooling.

Post-Cooling Stage

With time, the induced cracks during the heating and cooling stages start to be refilled with the new hydration products. Poon et al.[7] and Crook and Murray[9] have immersed concrete specimens in water after heating to 600 °C [1112 °F] and 500 °C [932 °F], respectively. These specimens experienced an accelerated re-curing that enhanced the strength regain. Sarshar and Khoury[6] used thermally stable firebrick aggregates to isolate the effect of aggregate and the cement paste. Harada et al.[8] used concrete mixes with siliceous aggregates and natural air drying where the air moisture was the only source affecting the re-curing process (relative humidity ≅ 65%). This experimental work is considered the most appropriate to simulate the behavior of fire damaged concrete in reality. Moreover, Harada et al.[8] reported $(f'_{cT})_t$ values at temperatures up to 500 °C [932 °F] and for a relatively long period of re-curing, one year, as shown in **Fig. 1a**. The observed

initial reduction in $(f'_{cT})_t$ after cooling is due to widening of the micro-cracks as explained in the cooling stage. The subsequent gradual recovery is caused by the C-S-H bond regeneration due to the continuous hydration. Based on test results by Harada et al.[8], Eq. (2) is developed to provide estimates for $(f'_{cT})_t$ following a fire event. Values of $(f'_{cT})_t$ estimated using Eq. (2) and assuming $(f'_{cT})_{t=0}$ is equal to the value reported by Harada at al.[8] are shown in Fig. 1a.

$$(f'_{cT})_{t=days} = (f'_{cT})_{t=0} + \left(28\times10^{-6}\, t^2 - 3\times10^{-3}\, t\right)(f'_c) \qquad \leq f'_c \qquad t \leq 90 \text{ days} \tag{2.a}$$

$$(f'_{cT})_{t=days} = 0.74(f'_{cT})_{t=0} + 0.01\left(\frac{a.t^b}{c^b + t^b}\right)(f'_c) \qquad \leq f'_c \qquad t > 90 \text{ days} \tag{2.b}$$

Where $a = 0.09\,T + 10.1$, $b = 0.0028\,T + 1.025$, $c = 0.336\,T - 3.5$, and T is in ^{o}C.

TENSILE STRENGTH OF CONCRETE

Flexural tensile strength of normal density concrete at ambient temperature (f_{cr}) can be calculated as $0.60\sqrt{f_c'}$ (Collins and Mitchell[12]) sections provide models to estimate the tensile strength of siliceous concrete during and after being exposed to fire temperatures.

Heating Stage

Although the research is limited in this area, Terro's model[3], Eq. (3), was recommended to predict the concrete tensile strength at elevated temperatures[2], $(f_{crT})_{t=0}$. Although f_{cr} at ambient temperatures is proportional to $\sqrt{f_c'}$, it was found that at elevated temperatures, $(f_{crT})_{t=0}$ is proportional to $(f'_{cT})_{t=0}$ This change in behavior might be attributed to the fact that the relationship between compressive and tensile behavior is changing at elevated temperatures.

$$(f_{crT})_{t=0} = f_{cr} \times \frac{(f'_{cT})_{t=0}}{f'_c} \tag{3}$$

Cooling and Post-Cooling Stages

Experimental work addressing concrete tensile resistance during these stages is missing in the literature. It is proposed to estimate $(f_{crT})_t$ using Eq. (3) after replacing $(f'_{cT})_{t=0}$ with $(f'_{cT})_t$.

INSTANTANEOUS STRESS RELATED COMPRESSIVE STRAIN

The value of the compressive strain at the peak stress (ε_{oT}) defines the compressive stress-strain relationship during the heating stage. While elevated temperatures result in increasing the value of ε_{oT}, preloading concrete during heating reduces the magnitude of this increase[2]. Terro's model[3], Eq. (4), was found to have good accuracy for estimating the value of ε_{oT} [2]. Variation of ε_{oT} with time is not addressed in this paper, as it has no effect on the concrete tensile behavior.

$$\varepsilon_{oT} = (50\lambda_L^2 - 15\lambda_L + 1).\varepsilon_{o1} + 20(\lambda_L - 5\lambda_L^2).\varepsilon_{o2} + 5(10\lambda_L^2 - \lambda_L)\times 0.002 \quad \geq 0.002$$
$$\text{where} \quad \varepsilon_{o1} = 2.05\times10^{-3} + 3.08\times10^{-6}.T + 6.17\times10^{-9}.T^2 + 6.58\times10^{-12}.T^3 \qquad (4)$$
$$\varepsilon_{o2} = 2.03\times10^{-3} + 1.27\times10^{-6}.T + 2.17\times10^{-9}.T^2 + 1.64\times10^{-12}.T^3$$

INITIAL MODULUS OF ELASTICITY

The initial modulus of elasticity at ambient temperature, E_{ci}, is defined as the slope of the compressive stress-strain relationship at zero strain. Its value during heating $(E_{ciT})_{t=0}$ and after cooling $(E_{ciT})_t$ is greatly affected by the preloading condition[2] and can be estimated at different fire stages using the models presented in the following sections.

Heating Stage

However great scatter was found in the experimental results addressing $(E_{ciT})_{t=0}$, the model proposed by Anderberg and Thelandersson [reported in 2], Eq. (5), was recommended to estimate $(E_{ciT})_{t=0}$ as it accounts for the effect of preloading[2]. It should be noted that by using this model the

effect of any discrepancy in the estimation of $(f'_{cT})_{t=0}$ and ε_{oT} will be carried over to the prediction of E_{ciT}.

$$(E_{ciT})_{t=0} = \frac{2 \times (f'_{cT})_{t=0}}{\varepsilon_{oT}} \tag{5}$$

Cooling and Post-Cooling Stages

As the concrete starts regaining its original compressive strength, $(E_{ciT})_t$ was found to start recovering its original value[8]. **Fig. 1b** shows the natural recovery of $(E_{ciT})_t$ of siliceous concrete as experimentally evaluated by Harada et al.[8] [reported in 1]. Due to the lack of analytical models, Eq. (6) was developed to estimate variation of $(E_{ciT})_t$ with time. The predictions of this equation, assuming $(E_{ciT})_{t=0}$ to be equal to the value reported by Harada et al., are shown in **Fig. 1b**.

$$(E_{ciT})_t = (E_{ciT})_{t=0} + E_{ci} \times \frac{0.8 \times t^{1.5}}{\left(\frac{3.2 \times 10^6}{T}\right) + t^{1.5}} \qquad \leq E_{ci} \tag{6}$$

YIELD STRENGTH OF REINFORCING BARS

The following sections trace changes in the yield strength of steel bars, f_y, after exposure to fire.

Heating Stage

Fire temperature reduces f_y and eliminates the yielding plateau observed in tensile tests of mild steel specimens. Due to large strains exhibited at elevated temperatures, yield stress at elevated temperatures (f_{yT}) is usually evaluated using the 1% or 2% proof stress rather than the conventional ambient value of 0.2%. Lie's model[1], Eq. (7), can be used to predict f_{yT}.

$$f_{yT} = \left[1 + \frac{T}{900 \times \ln\left(\frac{T}{1750}\right)}\right] \times f_y \qquad 0 < T \le 600\,^{\circ}\text{C} \qquad (7.a)$$

$$f_{yT} = \left[\frac{340 - 0.34 \times T}{T - 240}\right] \times f_y \qquad 600 < T \le 1000\,^{\circ}\text{C} \qquad (7.b)$$

Cooling and Post-Cooling Stages

Original yield and tensile strengths of typical hot-rolled steel bars fully recover on cooling after exposure to temperatures up to 600 °C [1112°F] [13, 14]. Folic et al.[15] validated this phenomenon by conducting tensile tests on samples of fire-damaged reinforcing steel bars. All the mechanical properties, including yield strength, tensile strength, modulus of elasticity, and maximum elongation, were fully recovered[15]. Reuse of reinforcing bars after exposure to fire depends on their buckling condition and should be assessed by visual inspection. For temperatures above 600 °C [1112 °F], the residual yield strength can be evaluated using linear interpolation by assuming 100% recovery for T=600 °C [1112 °F] and 70% recovery for T= 900 °C [1652 °F][13].

BOND STRENGTH OF REINFORCING BARS

The value of the bond strength between concrete and reinforcing bars is affected by the concrete type and the reinforcement surface condition (smooth, deformed or rusted) [16, 17]. **Figs. 2a** and **2b** show the experimentally evaluated bond strength at different temperatures for deformed and plain steel reinforcing bars, respectively. The figures also show the values of the residual bond strength. It is clear from the experimental results that cooling the specimens led to decreasing the bond strength[17]. This phenomenon might be attributed to widening of the micro cracks that was previously discussed in the concrete compressive strength section. The residual bond strength for deformed steel bars after exposure to elevated temperatures $(\tau_{uT})_{t=0}$ can be predicted using

Chiang and Tsai model[18]. Due to the complexity and impractically of this model, a simple model is proposed in this study, Eq. (8). Predictions of this model are shown in Fig. 2a.

$$(\tau_{uT})_{t=0} = \tau_{uo} + \tau_{uo}\left[0.01\times T - 1.7362\times 10^{-4}\times T^{2}\right]\times 10^{-2} \quad \geq 0.0 \tag{8}$$

Where τ_{u0} is the bond strength at ambient temperature

For plain steel bars, an approximate value of the reduced bond strength $(\tau_{uT})_{t=0}$ after exposure to elevated temperatures can be estimated using Xie and Qian model [reported in 17], Eq. (9). It was noted that this model is limited to T of 600 °C [1112 °F] as it shows an increase in the value of $(\tau_{uT})_{t=0}$ for higher temperatures. It is proposed to linearly decrease $(\tau_{uT})_{t=0}$ for higher temperatures until reaching a value of zero at T of 800 °C [1472 °F]. Predictions for this model are shown in Fig. 2b.

$$(\tau_{uT})_{t=0} = \tau_{uo}\left[2.7438\left(\frac{T}{100}\right)^{2} - 3.322\left(\frac{T}{10}\right) + 105.881\right]\times 10^{-2} \qquad T \leq 600\ ^{o}\text{C} \tag{9}$$

The residual bond strength, $(\tau_{uT})_t$, is expected to increase with time due to the continuous re-hydration of free lime during the post-cooling stage. As a result, the induced cracks between steel bars and adjacent concrete are filled by the new hydration products. $(\tau_{uT})_t$ may be therefore correlated to the compressive strength as given by equation 10.

$$(\tau_{uT})_{t} = (\tau_{uT})_{t=0} \times \frac{(f'_{cT})_{t}}{(f'_{cT})_{t=0}} \tag{10}$$

TENSILE STRESS-STRAIN RELATIONSHIP

The uniaxial stress-strain relationship for concrete in tension is usually modeled by a linear branch until reaching the cracking stress, f_{cr}. The modulus of elasticity of the linear branch can be taken equal to E_{ci}. After cracking, concrete tensile resistance results from the friction against the reinforcement and the tensile resistance of the pieces lying between the cracks[2]. One of the

popular models to represent this tension stiffening is that of Collins and Mitchell[12]. Equation 11 can be used to define the concrete tensile stress-strain relationship at ambient temperature[12].

$$\begin{aligned} f_t &= E_{ci} \times \varepsilon_c & \varepsilon_c &\le \frac{f_{cr}}{E_{ci}} \\ f_t &= \frac{\alpha_1 \alpha_2 f_{cr}}{1+\sqrt{500\varepsilon_c}} & \varepsilon_c &> \frac{f_{cr}}{E_{ci}} \end{aligned} \tag{11}$$

Where α_1 is a factor accounting for bond characteristics of reinforcing bars and can be taken equal to 1.0 or 0.7 for deformed or plain bars, respectively and α_2 is a factor accounting for type of loading and can be taken equal to 1.0 or 0.7 for short-term or sustained loading, respectively.

Heating Stage

Youssef and Moftah[2] proposed a similar model for the heating stage. The model utilizes the values evaluated for $(f_{crT})_{t=0}$, $(E_{ciT})_{t=0}$, and $(\tau_{uT})_{t=0}$, and is given by equation 12.

$$\begin{aligned} (f_{tT})_{t=0} &= (E_{ciT})_{t=0} \times \varepsilon_c & \varepsilon_c &\le \frac{(f_{crT})_{t=0}}{(E_{ciT})_{t=0}} \\ (f_{tT})_{t=0} &= \frac{\alpha_1 \alpha_2 \, (f_{crT})_{t=0}}{1+\sqrt{500\varepsilon_c}} \times \frac{(\tau_{uT})_{t=0}}{\tau_{uo}} & \varepsilon_c &> \frac{(f_{crT})_{t=0}}{(E_{ciT})_{t=0}} \end{aligned} \tag{12}$$

Post-Cooling Stage

Due to the lack of experimental work in this stage, it is proposed to use the same principles applied to the heating stage. Eq. (12) can be modified by replacing $(f_{tT})_{t=0}$, $(\tau_{uT})_{t=0}$, and $(E_{ciT})_{t=0}$ with $(f_{tT})_t$, $(\tau_{uT})_t$, and $(E_{ciT})_t$.

CASE STUDY

Siliceous concrete slabs sprayed at one side with a layer of a Thin Sprayed Liner (TSL) were exposed to fire at their protected side. Flexural tests were conducted on these fire-damaged slabs 85 days after fire exposure to examine their flexural behavior and to assess the effect of the TSL layer. Flexural tests were also conducted on slabs that were not exposed to fire. Slabs were divided into two groups. In the first group, slabs were positioned such that the TSL layer was in compression. This group included two slabs (14 and 16) that were not exposed to fire and three slabs (6, 7, and 9) that were fire tested. In the second group, slabs were positioned such that the TSL layer was in tension. This group included two slabs (4 and 5) that were not exposed to fire and four slabs (2, 8, 11, and 13) that were fire tested.

Specimens

The tested slabs, **Fig. 3**, had a width of 500 mm [19.7 in], an average length of 1219 mm [4 ft], and an average thickness of 53.8 mm [2.11 in]. The exact thickness for each of the tested slabs is given in the second column of **Tables 1** and **2**. The slabs were reinforced using 152 x 152 MW11.1 x MW11.1 Welded Wire Mesh (WWM) that was located at one side of the slabs. Tensile strength tests were conducted on three wires and an average tensile strength of 570 MPa was obtained. The TSL layer had an average thickness of 3 mm and was sprayed at the side having the WWM. Concrete having siliceous aggregate was used to construct the slabs. Each cubic meter [35.3 cubic feet] of concrete was made by mixing 470 kg [1036.2 1bs] of cement, 178 kg [392.4 1bs] of fine aggregates, 1.1 liter [0.039 cubic feet] of super plasticizer, and 1.5% air entraining agent. The 28 days concrete compressive strength was 53 MPa [7687 psi].

Fire Test

Two fire tests were conducted in accordance with CAN/ULC-S102-03[19]. Each test involved six concrete slabs that were arranged as a one continuous concrete slab as shown in **Fig. 4a**. Gas burners generated a continuous flame located 300 mm [11.8 in] from the end of the first slab. A constant airflow velocity of 1.2 m/sec [3.94 ft/sec] was created in the tunnel of the fire testing facility using forced ventilation. The slabs were instrumented with ceramic tip pyrometers at three sites (1, 2, 3) to determine the temperature distribution along the centerline of the tunnel. **Fig. 4b** shows the locations of the pyrometers at each of the three sites. Using these temperature measurements and assuming a linear interpolation/extrapolation, the average temperatures for each slab at points a, b, and d (T_a, T_b, and T_d) are reported in tables 1 and 2. **Fig. 4c** shows the variation of the temperature at point d with time for sites 1, 2, and 3.

Flexural Test setup

Fig. 5 shows the flexural test setup. Slabs were tested as simply supported with a span of 1000 mm [3.28 ft]. Two bars each with a length of 510 mm [1.67 ft] were used to create two hinged supports. The actuator load was transferred to the slab through a mechanism that allowed obtaining two lines of distributed loads at distances of 300 mm [l1.8 in] from each support. This included transferring the load to the concrete slab through an I beam, two tube sections, and two bars with length of 510 mm [1.67 ft]. Loading was applied by controlling the displacement at the midspan of the slab. A displacement rate of 0.5 mm/minute was used for all slabs.

Specimen preparation for flexural test

Following fire tests, slabs were shipped and stored in the Structures Laboratory at the University of Western Ontario. Instrumentations for the flexural tests included two 60 mm [2.4 in] strain

gauges to measure the maximum tensile and compressive strains and a Linear Variable Displacement Transducer (LVDT) to measure the mid-span deflection. The length of the strain gauges was chosen such that it is longer than 3 times the maximum aggregate size and thus allows measuring average concrete strains. Preparation of the slabs involved conducting the following steps: a) for group 1 of slabs: TSL material was removed at the locations of the two loading beams and the compressive strain gauge, b) for group 2 of slabs: TSL material was removed at the locations of the two supports and the tensile strain gauge. c) the concrete surface at the locations of the strain gauges were cleaned and smoothed, and d) two strain gauges were attached to the concrete surface at the midspan of the slabs using X60 adhesive mix.

EXPERIMENTAL RESULTS

This section summarizes the test results for group 1 (slabs with TSL on the compressive side) and group 2 (slabs with TSL on the tension side).

Slabs with TSL on the compression side

The two slabs (14 and 16) that were not subjected to fire behaved as expected showing a linear behavior and failing due to cracking of concrete. A single crack located close to the midspan was observed at failure. The relationships of load-midspan deflection, compressive strain-midspan deflection, tensile strain-midspan deflection, and a photograph of the crack pattern are shown in **Fig. 6** for slab 14. The point of cracking is marked on the graphs by the letter "C". Table 1 summarizes some of the important data for the two slabs at cracking: load (P_{cr}), stress (f_{cr}), tensile strain (ε_{cr}), compressive strain (ε_{comp}), and midspan deflection (δ_{cr}). Similar results are shown for the fire-damaged slabs 6, 7, and 9 in Table 1.

Slabs with TSL on the tension side

The two slabs (4 and 5) that were not subjected to fire behaved as expected showing better ductile behavior than slabs 14 and 16 of group 1. This improvement is mainly due to the WWM and TSL material that were located on the tension side. The experimental results for slab 4 are shown in **Fig. 7**. The load-midspan deflection relationship is found to be approximately linear up to cracking. Following cracking, the load dropped as the tensile forces were being transferred from the concrete to the WWM and the TSL material. Then the load started to increase again. Additional load drops were observed at onset of each additional crack. The slab appeared to be acting in a ductile manner until the WWM reached its strength and wires started fracturing one by one showing four drops in the load (marked with the letter "F"). Following fracture of all wires, the slab sustained about 25% of its ultimate capacity by utilizing the TSL material in tension. Table 2 summarizes some of the important data for the two slabs at cracking and at fracture of first steel wire. These data are: (1) at cracking: P_{cr}, f_{cr}, ε_{cr}, ε_{comp}, and δ_{cr}, and (2) at fracture of first steel wire: number of cracks observed, compressive strain (ε_f), and midspan deflection (δ_f). The results show that stresses and strains at cracking were similar to those of group 1 of undamaged slabs. Similar results are shown for the fire-damaged slabs 2, 8, 11, and 13 in Table 2. **Fig. 8** shows the test results for fire-damaged slab 2. TSL layer was not effective in resisting tensile loads as it was exfoliated into loose spongy form when it was subjected to fire temperatures.

DISCUSSION

The temperatures measured during the fire tests showed that the TSL material has significantly reduced the temperature experienced by the concrete surface from a maximum value of about 500^{o}C [932 ^{o}F] (temperature at point e) to a maximum value of about 150^{o}C [302 ^{o}F] (temperature at concrete surface between points d and e). This reduction minimized the effect of

fire on the properties of concrete and WWM. The following sections provide discussion of proposed analytical models in terms of the experimental results.

Slabs with TSL on the compression side

For group 1 tests (TSL and the WWM are in compression), the slab flexural behavior is similar to that of plain concrete. Table 1 shows that the temperatures at the tension side of the slabs are close to the ambient temperature. The two undamaged slabs (14 and 16) cracked at an average tensile stress of $0.60\sqrt{f_c'}$ MPa, which matches the proposed value. The average initial modulus of elasticity of the two slabs can be experimentally evaluated as $\frac{f_{cr}}{\varepsilon_{cr}}$ and is found equal to 27,221 MPa. The compressive strain at cracking shows that concrete did not reach the strain defining the peak stress as the behavior was mainly controlled by the concrete tensile capacity.

The results show that the fire-damaged slabs cracked at an average stress of $0.80\sqrt{f_c'}$ suggesting that they were able to sustain higher tensile stresses than undamaged slabs. It is known that low increase of temperatures might enhance concrete residual properties[5, 20]. This increase is mainly attributed to the initiation of the re-hydration process. Another factor that might have affected the results is the method of testing. During fire testing, slabs were oriented such that the TSL material is at the bottom and directly exposed to fire. The top side of the slab was subjected to compressive strains due to own-weight of the slab and compressive thermal strains resulting from the temperature difference between top and bottom of the slab. These compressive strains might have increased due to transient creep effects. After cooling of the slabs, these compressive strains likely did not go back to zero resulting in a permanent residual compressive strain. In flexural tests, slabs were oriented such that the side with permanent compressive strains is on the tension

side. Thus, higher forces were required to cause cracking. This reason is supported by the increase in cracking strain noted in slab 9. The initial modulus of elasticity of slab 9 is found equal to 30,947 MPa. The increase in the initial modulus suggests that the tensile strength have increased by 14% due to the increase of concrete strength and by 17% due to the generated transient strain during fire test.

Slabs with TSL on the tension side

For group 2 tests, TSL and WWM are in tension; the slab flexural behavior is affected by the tensile capacity of the WWM and the TSL material. The reinforcement area provided by the WWM in the slab section is 44.4 mm^2 (0.00165 of the average slab area). This reinforcement ratio is lower than the minimum ratio (0.002) specified in A23.3-04[21]. The two undamaged slabs (4 and 5) cracked at an average tensile stress of $0.56\sqrt{f_c'}$ MPa. The average initial modulus of elasticity of slab 5 is found equal to 24,276 MPa. The compressive strain at cracking shows that concrete did not reach the strain defining the peak stress. The ratio of maximum load observed , P_u, and P_{cr} is also given in Table 2. The two slabs sustained loads that are about 50% higher than the cracking load. The tensile capacity of the wire mesh was found to be equivalent to the pre-cracking tensile capacity of the concrete section. The additional 50% increase in the load is corresponding to the tensile capacity of the TSL layer.

As the TSL material protected the slabs from the fire temperature, the reduction in the compressive capacity of the slabs is not expected to exceed about 10%. Values provided in Table 2 show that fire damaged slabs cracked at an average stress of $0.67\sqrt{f_c'}$, which is slightly higher than the cracking stress of undamaged slabs. The cracking strain for these slabs was similar to the undamaged slabs. Again, the low rise of temperature might have increased the concrete residual

strength[5, 20]. The average initial modulus of elasticity for these slabs is found equal to 29,880 MPa. The percentage increase in tensile resistance is almost equal to the percentage increase in the initial modulus proving that the concrete strength has increased. Following cracking, the behavior of these slabs was mainly dependent on the WWM. For the fire-damaged slabs, the TSL layer was not effective as discussed in the experimental part. For some of the slabs (8 and 11), the increase in the WWM temperature has resulted in lowering its strength and thus, a reduced post-cracking load carrying capacity was observed. Elevated temperature has also decreased the deflection at which the fracture of the steel wires occurs. The compressive strain at fracture of the wire mesh shows that concrete did not reach the strain defining the peak stress.

Table 3 summarizes the expected mechanical properties for the fire-damaged slabs 2, 8, 11, and 13 using the models presented in this paper. The estimated concrete cracking stresses at different temperatures were compared with the experimental results obtained from flexure test. It can be concluded that the proposed models provides conservative estimates. According to the predicted values, concrete bond strength and modulus of elasticity experienced significant deterioration. **Fig. 9** shows tensile stress-strain relationships at ambient temperature and after exposure to temperatures 500 ^{o}C [932 ^{o}F] (assuming that TSL was not applied) and 168 ^{o}C [302 ^{o}F] (Slab 8). The figure shows the significant advantage of using the TSL layer. It also explains the sharp drop noted upon cracking of all the tested slabs.

CONCLUSIONS

The main objective of this paper is to assess the flexural behavior of siliceous concrete slabs after exposure to fire temperatures. For unreinforced or lightly reinforced slabs, this behavior is controlled by the concrete tensile behavior. The first part of the paper presents a set of analytical models to predict properties affecting the concrete tensile behavior during or after exposure to

elevated temperatures. These models are either collected from the literature or developed based on the available experimental results. The developed models are mainly covering the post-cooling stage as previous research in this area was found to be limited. The properties investigated include concrete compressive strength, concrete tensile strength, concrete compressive strain at peak stress, and bond strength of reinforcing bars. These properties were later used to formulate tensile stress-strain relationships at different fire stages.

The second part of the paper presents a case study where 11 concrete slabs are covered with a TSL material. Seven of them were exposed to elevated temperatures at the TSL protected side. Following fire testing, the slabs were tested in flexure with the TSL material either in compression or in tension. Based on the presented material models and the case study, the following conclusions can be drawn.

1. The reduction of fire temperatures experienced by the concrete slab due to the TSL material reduced the fire effect on the properties of the concrete slab and its reinforcement. Additional fire tests should be conducted to validate the effectiveness of the TSL layer for temperatures higher than 500 ^{o}C [932 ^{o}F].
2. Undamaged concrete slabs (slabs that were not exposed to fire): the flexural behavior of concrete slabs that were tested with the TSL layer on the compressive side was mainly linear. Failure occurred at the onset of concrete cracking and the TSL layer had no effect on the flexural behavior of these slabs. Slabs tested with TSL layer on the tensile side showed a better behavior due to the tensile resistance provided by the steel wire mesh and the TSL layer. Failure occurred due to fracture of the steel wires. TSL layer has resulted in increasing the capacity of the slabs by about 50%. Changing the slab dimensions, reinforcement ratio, TSL thickness, or TSL properties might affect this ratio.

3. Fire tested concrete slabs with TSL layer on the compressive side: these slabs performed in a similar manner as compared to the undamaged slabs. Failure occurred due to cracking of concrete. It can be stated that the effect of the conducted fire tests on the flexural behavior of these slabs was minimal.
4. Fire tested concrete slabs with TSL layer on the tensile side: the behavior of these slabs was showing some ductility similar to the undamaged slabs. This ductility was mainly due to the steel wire mesh. The TSL layer was ineffective as it was exfoliated into loose spongy form when it was subjected to fire temperatures. The post-cracking strength for some of these slabs was reduced as a result of reduction of the tensile capacity of the wire mesh.
5. The proposed models resulted in conservative estimations for the tensile strength. Additional tests are needed to further improve and validate these models. These tests should present data for different temperatures, preloading, slab thickness, reinforcement ratio, recovery period, cooling method and environmental conditions.

ACKNOWLEDGMENTS

The authors gratefully acknowledge the contributions of Professor K.Y. Lo of the University of Western Ontario to the experimental study presented in this paper. Funding was provided by the Natural Sciences and Engineering Research Council of Canada (NSERC) and the Toronto Transit Commission (TTC), Toronto, Ontario.

NOTATIONS:

a, b, c = constants describing the regain of compressive strength with time after fire exposure.

E_{ci} = initial modulus of elasticity at ambient temperature.

$(E_{ciT})_{t=0}$ = initial modulus of elasticity at elevated temperature.

$(E_{ciT})_t$ = initial modulus of elasticity at time t.

f_c = compressive stress in concrete.

f'_c = concrete compressive strength at ambient temperature.

$(f'_{cT})_{t=0}$ = concrete compressive strength at elevated temperature.

$(f'_{cT})_t$ = concrete compressive strength at time t.

f_{cr} = cocncrete tensile strength at ambient temperature.

$(f_{crT})_{t=0}$ = cocncrete tensile strength at elevated temperature.

$(f_{crT})_t$ = tensile resistance of concrete at time t.

f_t = tensile stress in concrete.

f_y = yield strength of reinforcing bars at ambient temperature.

f_{yT} = yield strength of reinforcing bars at elevated temperature.

P_u = ultimate load sustained by the tested concrete slabs.

t = time after fire exposure in days.

T = fire temperature in degree celsius [$T\,^{o}\text{C} = (T\,^{o}\text{F} - 32)\ 5/9$] .

T_d, T_b, T_a = temperature at locations d, b, and a for the tested slabs.

α_1 = factor to account for bond characteristics of reinforcing bars on the concrete tension stiffeneing.

α_2 = factor to account for type of loading on the concrete tension stiffening.

ε_{comp} = maximum compressive strain in the tested slabs.

ε_f = strain at fracture of first steel wire of the tested slabs.

ε_t = concrete tensile strain.

$\varepsilon_{o1}, \varepsilon_{o2}$ = strain at stress level λ_L of 0.0 and 0.1 respectively.

ε_{oT} = strain at maximum stress at elevated temperatures.

λ_L = preloading stress level $\frac{f_c}{f'_c}$.

τ_{uo} = bond strength at ambient temperature.

$(\tau_{uT})_{t=0}$ = residual bond strength after exposure to elevated temperatures.

$(\tau_{uT})_t$ = bond strength at time *t*.

δ_{cr} = midspan deflection at cracking of the tested slabs.

δ_f = midspan deflection at fracture of first steel wire of the tested slabs.

REFERENCES

1. Lie, T.T., "Structural Fire Protection," ASCE Manuals and Reports on Engineering Practice No. 78, New York, NY, 1992, 241 pp.
2. Youssef, M.A., and Moftah, M., "General Stress-Strain Relationship for Concrete at Elevated Temperatures," Engineering Structures, V. 29, Issue 10, 2007, pp. 2618-2634.
3. Terro, M.J., "Numerical Modeling of the Behavior of Concrete Structures in Fire," ACI Structural Journal, V. 95, No. 2, 1998, pp. 183-193.
4. Hertz, K.D., "Concrete Strength for Fire Safety Design," Magazine of Concrete Research, V. 57, No. 8, 2005, pp. 445-453.
5. Khoury, G.A., "Compressive Strength of Concrete at High Temperatures: a Reassessment," Magazine of Concrete Research, V. 44, No. 161, 1992, pp. 291-309.
6. Sarshar, R., and Khoury, G.A., "Material and Environmental Factors Influencing the Compressive Strength of Unsealed Cement Paste and Concrete at High Temperatures," Magazine of Concrete Research, V. 45, No. 162, 1993, pp. 51-61.
7. Poon, C., Azhar, S., Anson, M., and Wong, Y., "Strength and Durability Recovery of Fire-Damaged Concrete After Post-Fire-Curing," Cement and Concrete Research, V. 31, No.9, 2001, pp. 1307-1318.
8. Harada, T., Takeda, J., Yamane, S., and Furumura, F., "Strength, Elasticity and Thermal Properties of Concrete Subjected to Elevated Temperatures," ACI Special Publication 34, Concrete for Nuclear Reactors, Detroit, MI, 1972, pp. 377-406.
9. Crook, D.N., and Murray, M.J., "Regain of Strength After Firing of Concrete," Magazine of Concrete Research, V. 22, No. 72, 1970, pp. 149-154.
10. Abrams, M.S., "Compressive Strength of Concrete at Temperatures to 1,600 ^{o}F," ACI Special Publication 25, Temperature and Concrete, Detroit, MI, 1971, pp. 33-59.

11. ASTM C78, "Standard Test Method for Flexural Strength of Concrete (Using Simple Beam with Third-Point Loading)," American Society for Testing and Materials Standard Practice C78, ASTM, West Conshohocken, PA, 2007.
12. Collins, M.P., and Mitchell, D., "Prestressed Concrete Basics," Ottawa, ON, Canada: Canadian Prestress Concrete Institute; 1987.
13. Neves, I.C., Rodrigues, J., and Loureiro, A., "Mechanical Properties of Reinforcing and Prestressing Steels After Heating," Journal of Materials in Civil Engineering, V. 8, No. 4, 1996, pp. 189-194.
14. Concrete Society, "Assessment of Fire-Damaged Concrete Structures and Repair by Gunite," Technical Report No. 15, 1978, London, England.
15. Folic, R., Radonjanin, V., and Malesev, M., "The Assessment of Structure of Novi Sad Open University Damaged in a Fire," Construction and Building Materials, V. 16, No. 7, 2002, pp. 427-440.
16. Malhotra, H.L., "Design of Fire-Resisting Structures," London: Surrey University Press; 1982, pp. 45-85.
17. Xiao, J., and König, G., "Study on Concrete at High Temperature in China-an Overview," Fire Safety J., V. 39, No. 1, 2004, pp. 89-103.
18. Chiang, C., and Tsai, C., "Time-Temperature Analysis of Bond Strength of a Rebar After Fire Exposure," Cement and Concrete Research, V. 33, No.10, 2003, pp. 1651-1654.
19. CAN/ULC-S102-03, "Method of Test for Surface Burning Characteristics of Building Materials and Assemblies," Underwriters' Laboratories of Canada, Toronto, Ontario, 2003, 28 pp.
20. CPCI, "Design Manual: Precast and Prestressed Concrete," Canadian Precast/Prestressed Concrete Institute, Ottawa, Ontario, 2007.

21. CDH, “Concrete Design Handbook,” Cement Association of Canada, Ottawa, Ontario, 2006.

TABLES AND FIGURES

List of Tables:

List of Figures:

Table 1 - Slabs with TSL on the compression side

Slab	Thickness mm [in]	Temperature °C [°F]			at cracking					Number of cracks
		T_d	T_b	T_a	P_{cr} kN [kips]	f_{cr} N/mm^2 [psi]	ε_{cr}	ε_{comp}	δ_{cr} mm [in]	
14	54.33 [2.14]	NA	NA	NA	6.9 [1.6]	4.21 [611]	0.000151	0.000124	1.20 [0.05]	1
16	55.00 [2.17]	NA	NA	NA	6.4 [1.4]	3.81 [553]	0.000170	0.000136	0.78 [0.03]	1
6	51.83 [2.04]	30 [86]	25 [77]	20 [68]	7.7 [1.7]	5.16 [748]	0.000259	0.000170	1.28 [0.05]	1
7	55.50 [2.19]	30 [86]	25 [77]	20 [68]	9.4 [2.1]	5.49 [796]	0.000393	0.000127	0.75 [0.03]	1
9	52.33 [2.06]	40 [104]	40 [104]	25 [77]	9.0 [2.0]	5.92 [859]	0.000201	0.000159	1.29 [0.05]	1

Table 2 - Slabs with TSL on the tension side

Slab	Thickness mm [in]	Temperature °C [°F]			At cracking					P_u/P_{cr}	At fracture of 1st steel wire		
		T_d	T_b	T_a	P_{cr} kN [kips]	f_{cr} N/mm^2 [psi]	ε_{cr}	ε_{comp}	δ_{cr} mm [in]		Number of cracks	ε_f	δ_f mm [in]
4	53.17 [2.09]	NA	NA	NA	5.6 [1.3]	3.57 [518]	0.000115	0.000111	1.13 [0.04]	1.54	5	0.001801	33.87 [1.3]
5	52.83 [2.08]	NA	NA	NA	6.0 [1.3]	3.87 [561]	0.000174	0.000183	1.17 [0.05]	1.43	3	0.000186	35.05 [1.4]
2	56.83 [2.24]	90 [194]	65 [149]	35 [95]	7.9 [1.8]	4.40 [638]	0.000195	0.000140	1.01 [0.04]	1.11	2	0.000185	26.59 [1.0]
8	53.83 [2.12]	135 [275]	65 [149]	50 [122]	7.0 [1.6]	4.35 [631]	0.000169	0.000180	1.24 [0.05]	1.04	2	0.000153	28.29 [1.1]
11	52.50 [2.07]	105 [221]	60 [140]	50 [122]	7.2 [1.6]	4.70 [682]	0.000165	0.000150	1.05 [0.04]	1.00	1	0.000086	19.43 [0.8]
13	53.83 [2.12]	70 [158]	50 [122]	30 [86]	7.6 [1.7]	4.72 [685]	0.000137	0.000130	1.37 [0.05]	1.07	2	0.000140	16.60 [0.7]

1

2 **Table 3 – Application of proposed models to the tested slabs**

		Analytical at t = 85 days						Experimental	
Slab	Surface Temperature °C [°F]	$\frac{(f'_{cT})_t}{f'_c}$	$\frac{(E_{ciT})_t}{E_{ciT}}$	$\frac{(\tau_{uT})_t}{\tau_{uo}}$	$\frac{f_{yT}}{f_y}$	$\frac{(f_{crT})_t}{f_{cr}}$	$(f_{crT})_t$ N/mm^2 [psi]	$(f_{crT})_t$ N/mm^2 [psi]	Error %
2	103 [218]	0.924	0.821	0.706	0.960	0.924	4.04 [586]	4.40 [638]	-8
8	168 [334]	0.895	0.715	0.546	0.920	0.895	3.91 [567]	4.35 [631]	-10
11	122 [251]	0.917	0.790	0.657	0.949	0.917	4.01 [582]	4.70 [682]	-15
13	76 [169]	0.933	0.864	0.778	0.973	0.933	4.08 [592]	4.72 [685]	-14

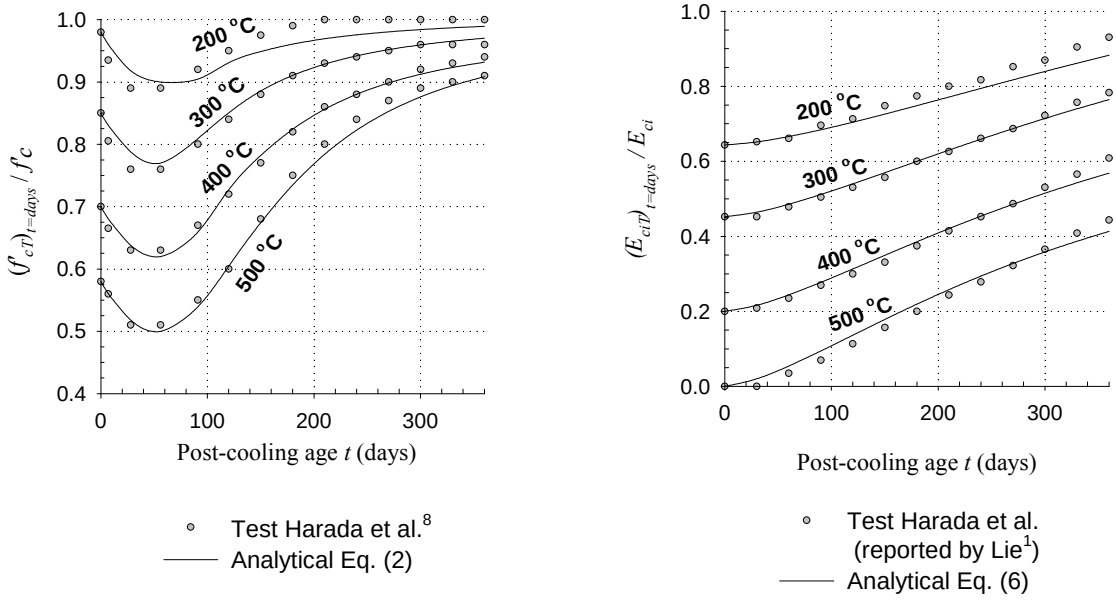

a) Compressive strength b) Modulus of Elasticity

Fig. 1–Recovery of fire-damaged concrete properties with time.
($T\ ^oF = 1.8T\ ^oC + 32$)

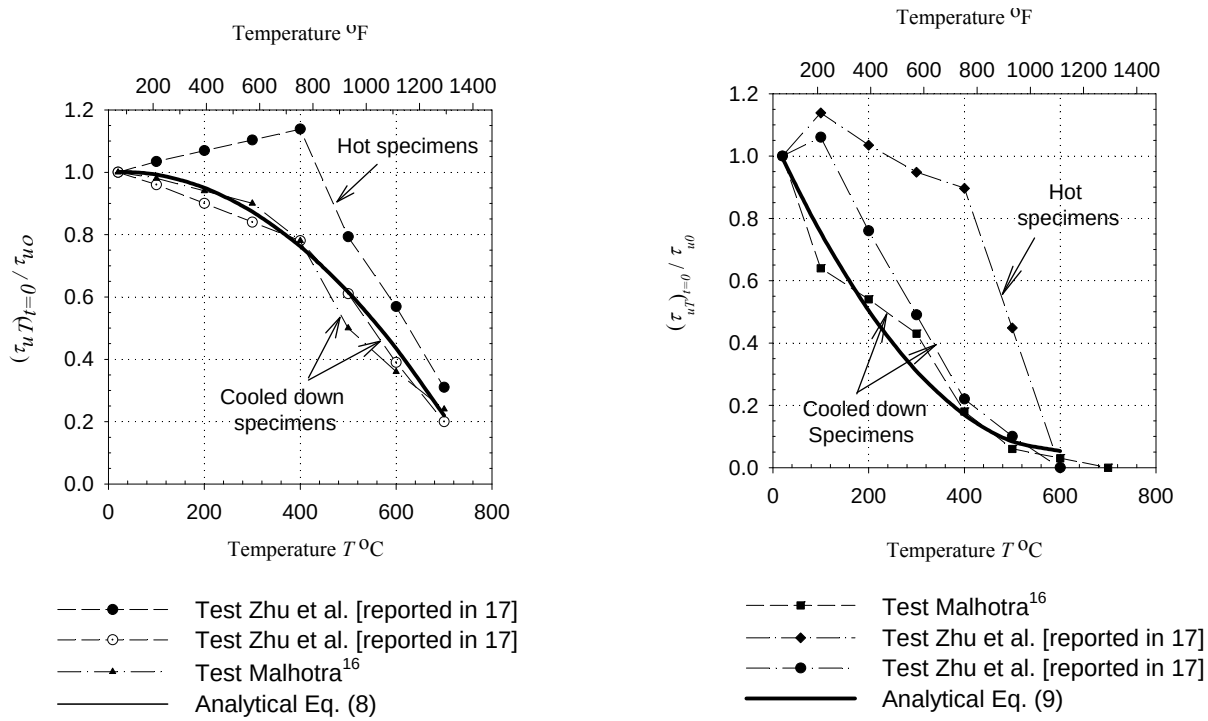

a) Deformed steel bars b) Plain steel bars

Fig. 2–Bond strength at elevated temperatures.

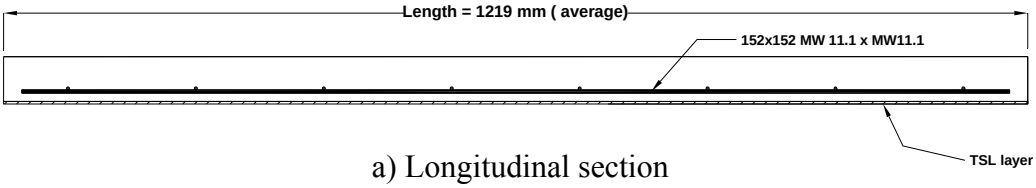

a) Longitudinal section

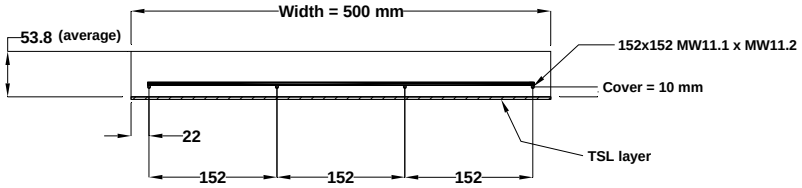

a) Transverse section

Fig. 3–Dimensions and reinforcement of concrete slabs.
(1 inch = 25.4 mm)

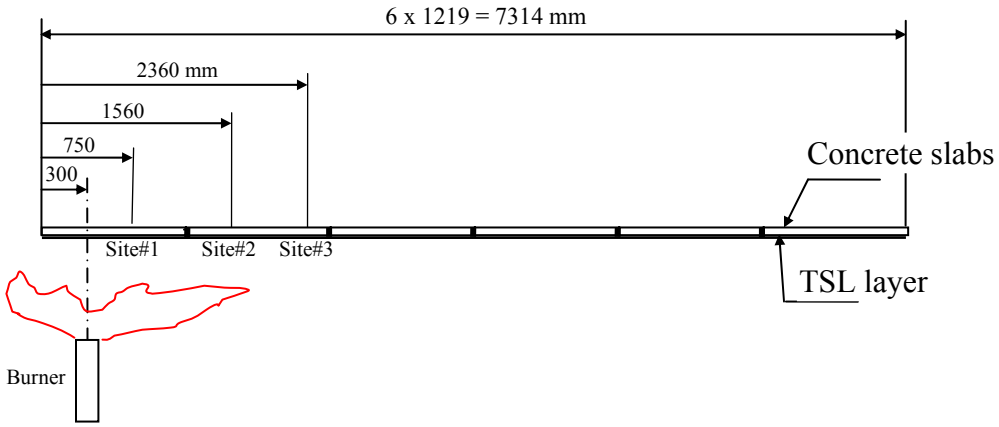

a) General Layout

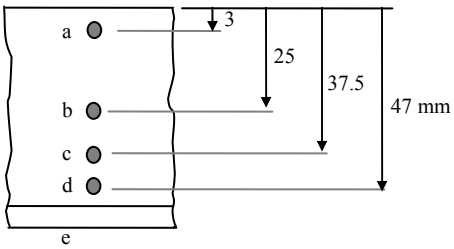

b) Location of pyrometers at sites 1, 2, and 3.

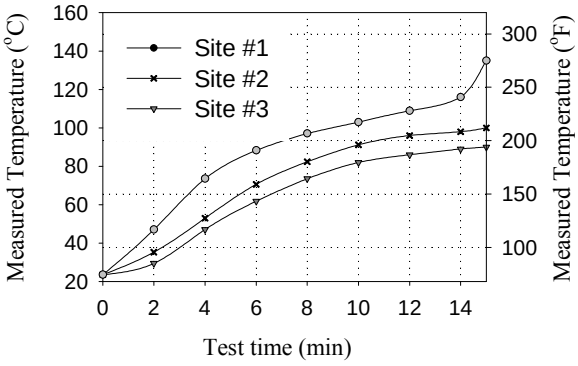

c) Temperatures at point d

Fig. 4–Slabs during fire testing
(1 inch = 25.4 mm)

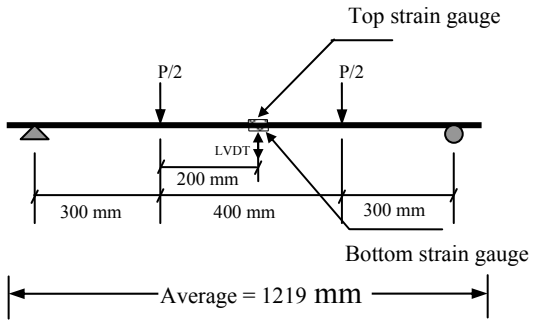

a) Schematic

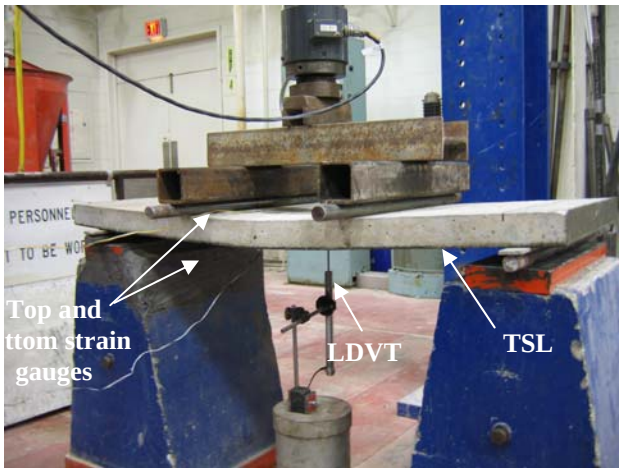

b) photograph

Fig. 5 – Flexural test setup.
(1 inch = 25.4 mm)

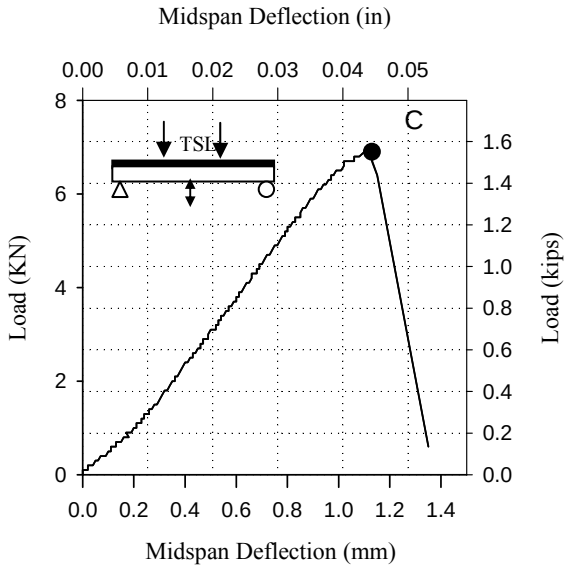

a) Load-midspan deflection relationship

b) crack pattern (bottom view of the slab)

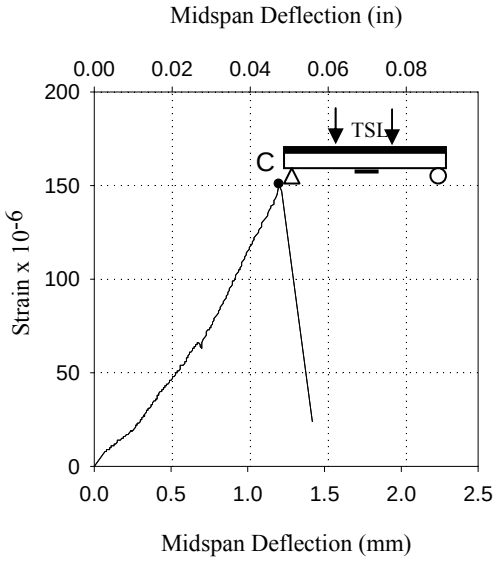

c) Midspan deflection-tensile strain relationship

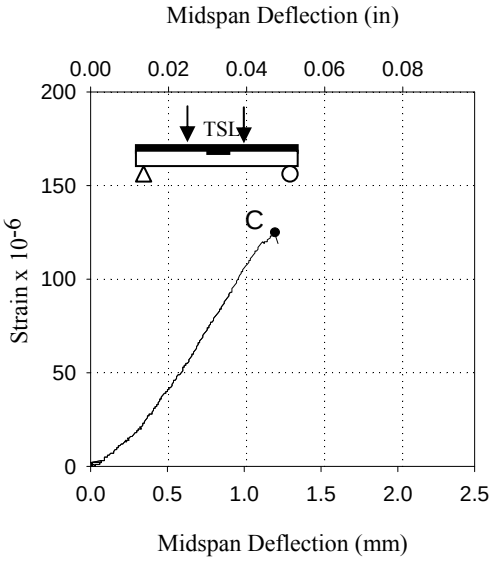

d) Midspan deflection-compressive strain relationship

Fig. 6–Results of flexural test of slab 14 with TSL on the compressive side.

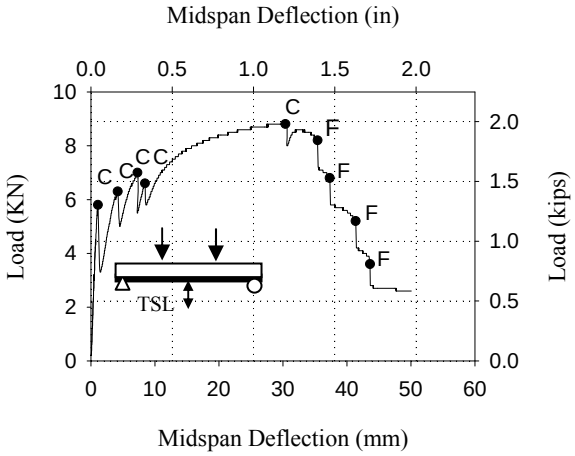

a) Load-midspan deflection relationship

b) crack pattern (side view of the slab)

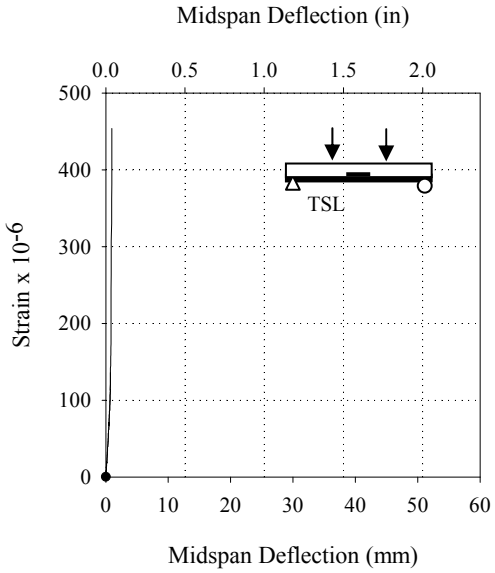

c) Midspan deflection-tensile strain relationship

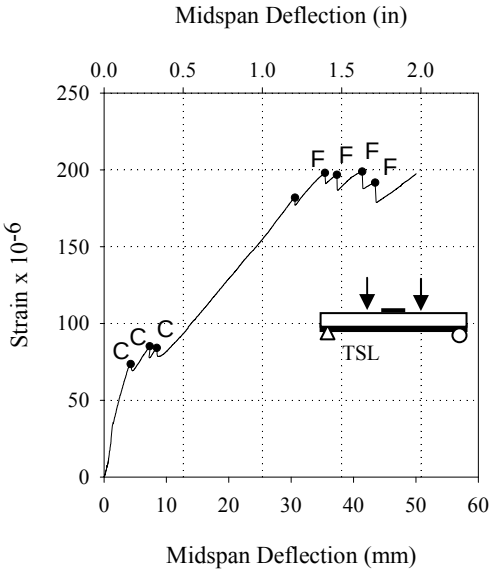

d) Midspan deflection-compressive strain relationship

Fig. 7–Results of flexural test of slab 4 with TSL on the tensile side.

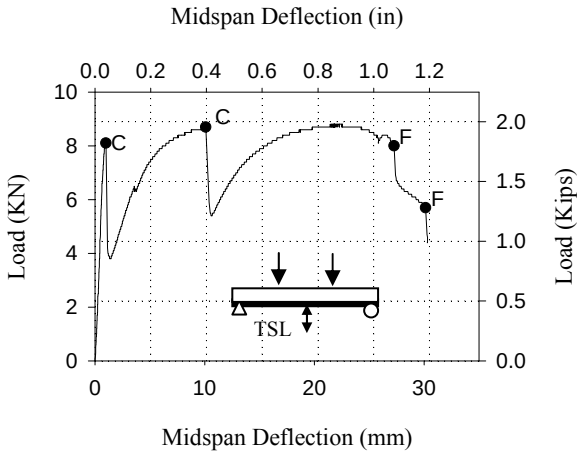

a) Load-midspan deflection relationship

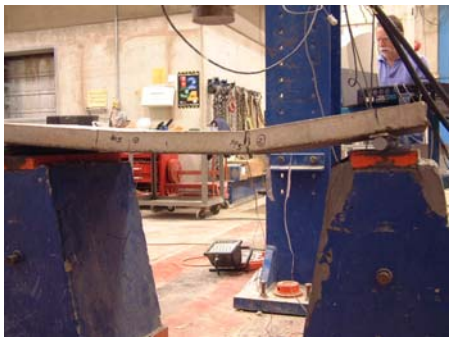

b) Deflected shape of the slab

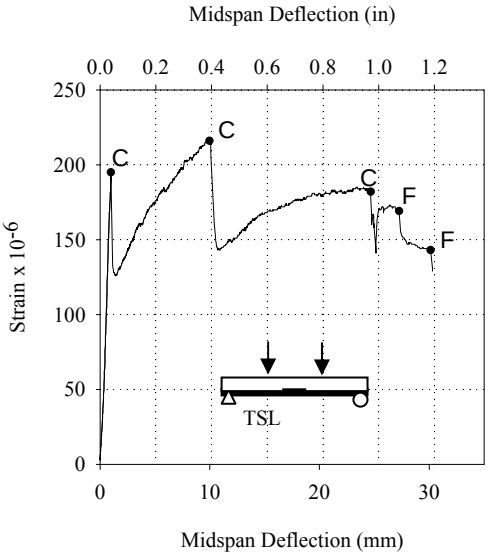

c) Midspan deflection-tensile strain relationship

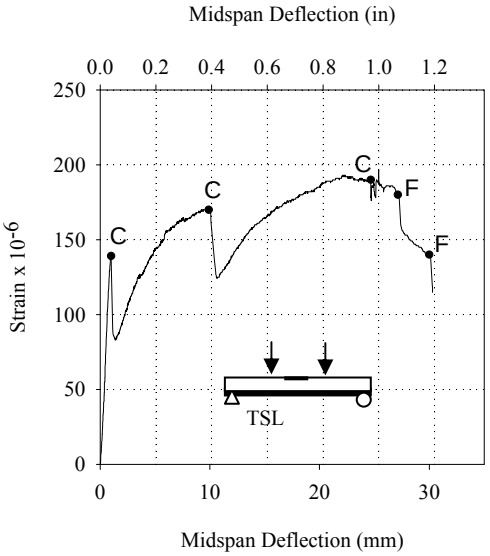

d) Midspan deflection-compressive strain relationship

Fig. 8–Results of flexural test of fire damaged slab 2 with TSL on the tensile side.

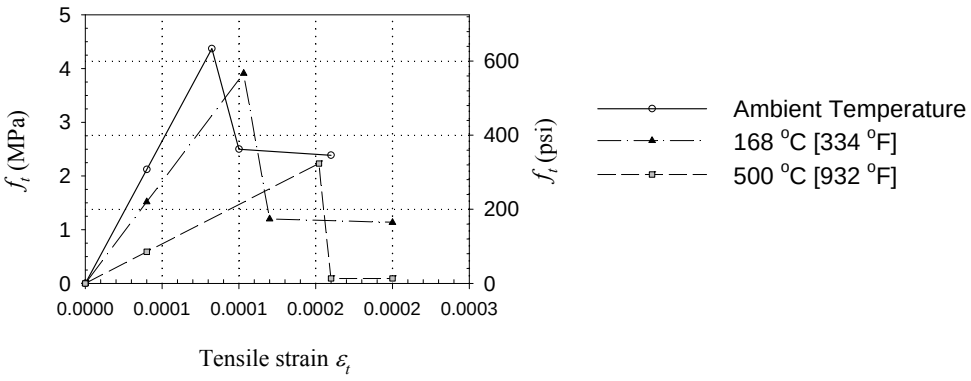

Fig. 9–Proposed tensile stress-strain relationship for slab 8.